

Experimental Characterization and First-Principles Understanding on the Structure of Zr-doped UO₂

15th November 2019

Jeongmook Lee¹, Choa Kwon², Jandee Kim¹, Young-Sang Youn³,
Jong-Yun Kim¹, Byungchan Han², Sang Ho Lim¹

¹Nucelar Chemistry Research Team, KAERI

²Department of Chemical and Biomolecular Engineering,
Yonsei University

³Department of Chemistry, Yeungnam University



CONTENTS

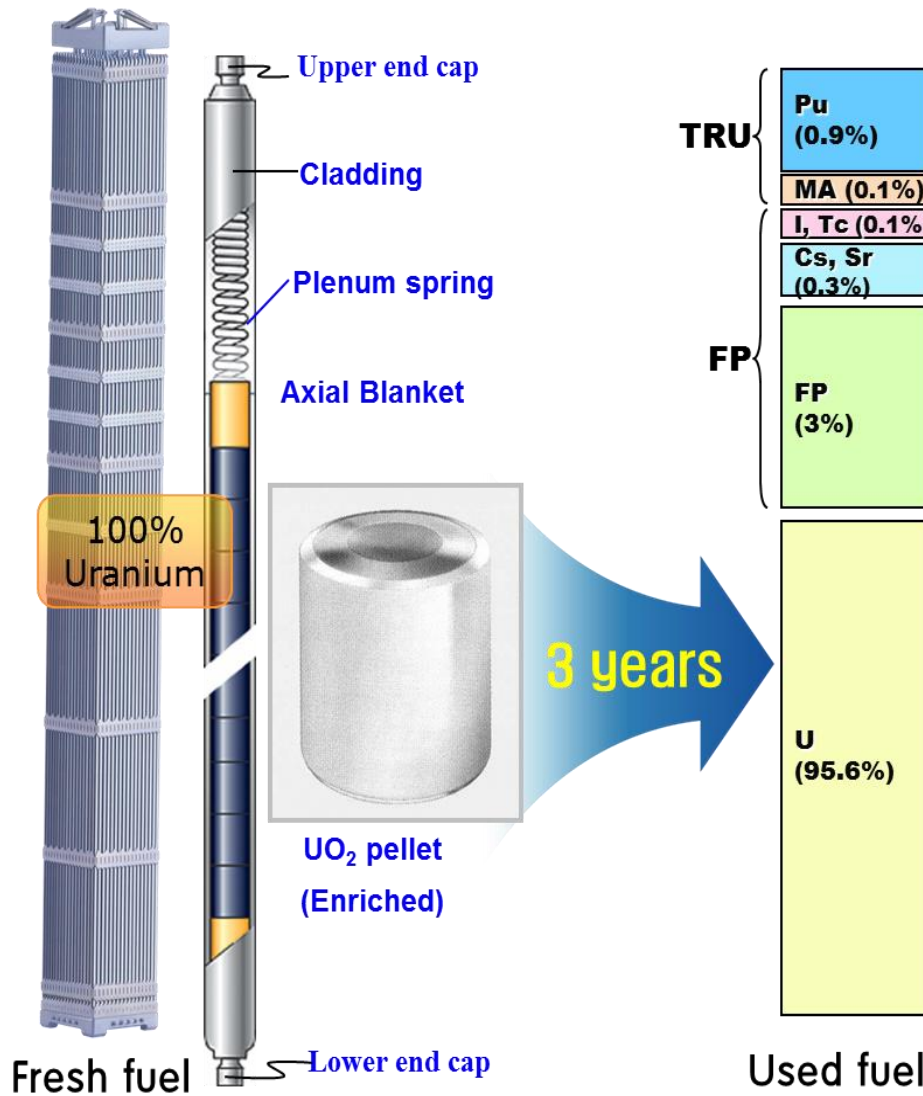
- I Introduction**
- II Experiment**
- III Results & Discussion**
- IV Summary**

I. Introduction



I. Introduction

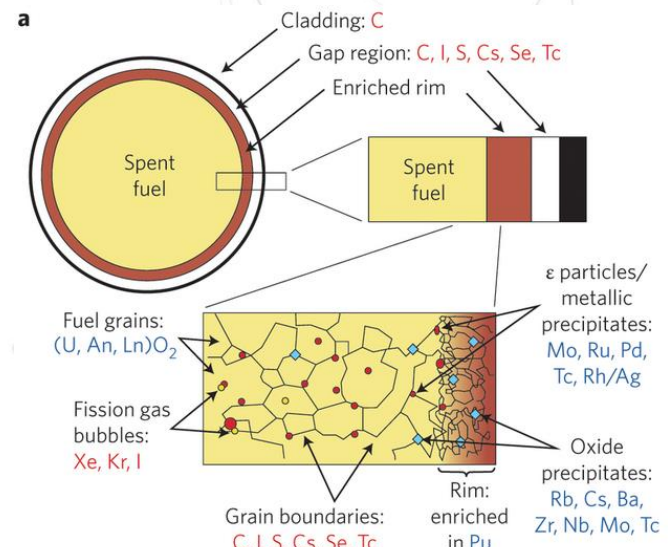
Distribution of fission products and actinides after irradiation



Chemical inventory for HBU SNF in CORE and OUT regions.

Element	HBU-CORE ($\mu\text{g/g}$)	HBU-OUT ($\mu\text{g/g}$)
Rb	500 ± 100	600 ± 120
Sr	800 ± 160	800 ± 160
Y	310 ± 130	340 ± 150
Zr	6300 ± 1300	7900 ± 1600
Mo	5900 ± 1180	8000 ± 1600
Tc	1300 ± 260	1600 ± 300
Ru	4400 ± 880	5300 ± 1100
Rh	650 ± 130	800 ± 160
Cs	3800 ± 200	4800 ± 240
La	2000 ± 400	2300 ± 500
Nd	7000 ± 1400	8000 ± 1600
U	780000 ± 78000	770000 ± 77000
Np	810 ± 160	760 ± 150
Pu	8000 ± 1600	11000 ± 2200
Am	840 ± 170	1200 ± 240
Cm	290 ± 60	460 ± 90

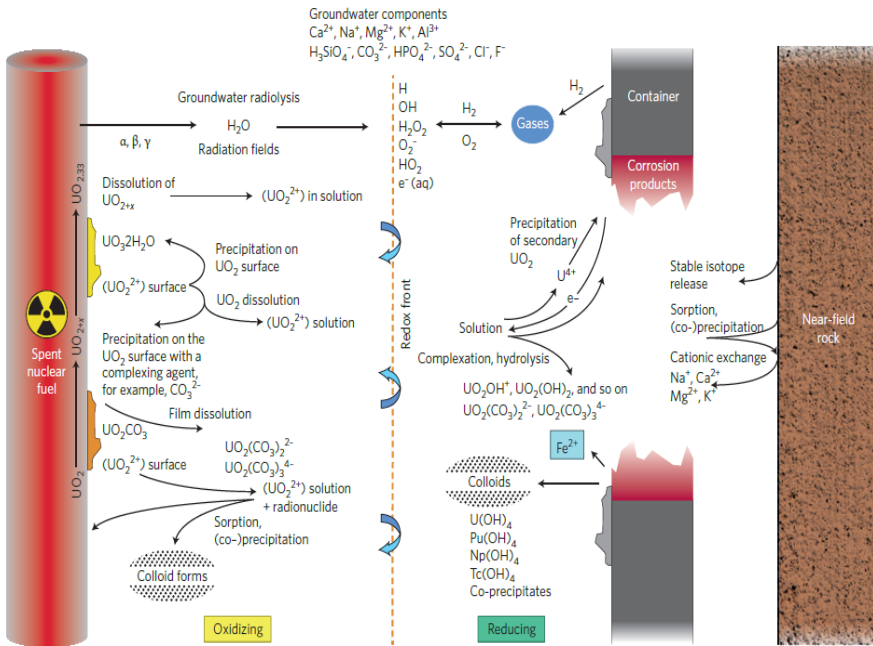
D. Serrano-Purroy *et al.*, J. Nucl. Mater. 427 (2012) 249-258



R.C. Ewing, Nature Mater. 14 (2015) 252-257

J. Bruno *et al.*, Elements 2 (2006) 343-349

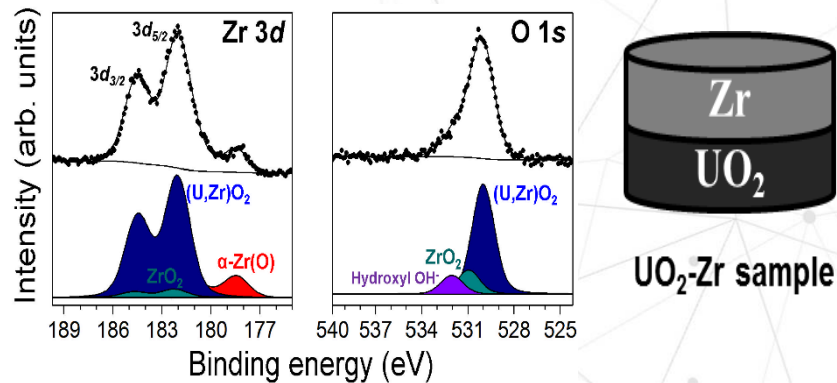
I. Introduction



Chemical inventory for HBU SNF in CORE and OUT regions.

Element	HBU-CORE ($\mu\text{g/g}$)	HBU-OUT ($\mu\text{g/g}$)
Rb	500 ± 100	600 ± 120
Sr	800 ± 160	800 ± 160
Y	310 ± 130	340 ± 150
Zr	6300 ± 1300	7900 ± 1600
Mo	5900 ± 1180	8000 ± 1600
Tc	1300 ± 260	1600 ± 300
Ru	4400 ± 880	5300 ± 1100
Rh	650 ± 130	800 ± 160
Cs	3800 ± 200	4800 ± 240
La	2000 ± 400	2300 ± 500
Nd	7000 ± 1400	8000 ± 1600
U	780000 ± 78000	770000 ± 77000
Np	810 ± 160	760 ± 150
Pu	8000 ± 1600	11000 ± 2200
Am	840 ± 170	1200 ± 240
Cm	290 ± 60	460 ± 90

D. Serrano-Purroy *et al.*, J. Nucl. Mater. 427 (2012) 249-258



Y.-S. Youn *et al.*, Bull. Korean Chem. Soc. 36 (2015) 2068-2072

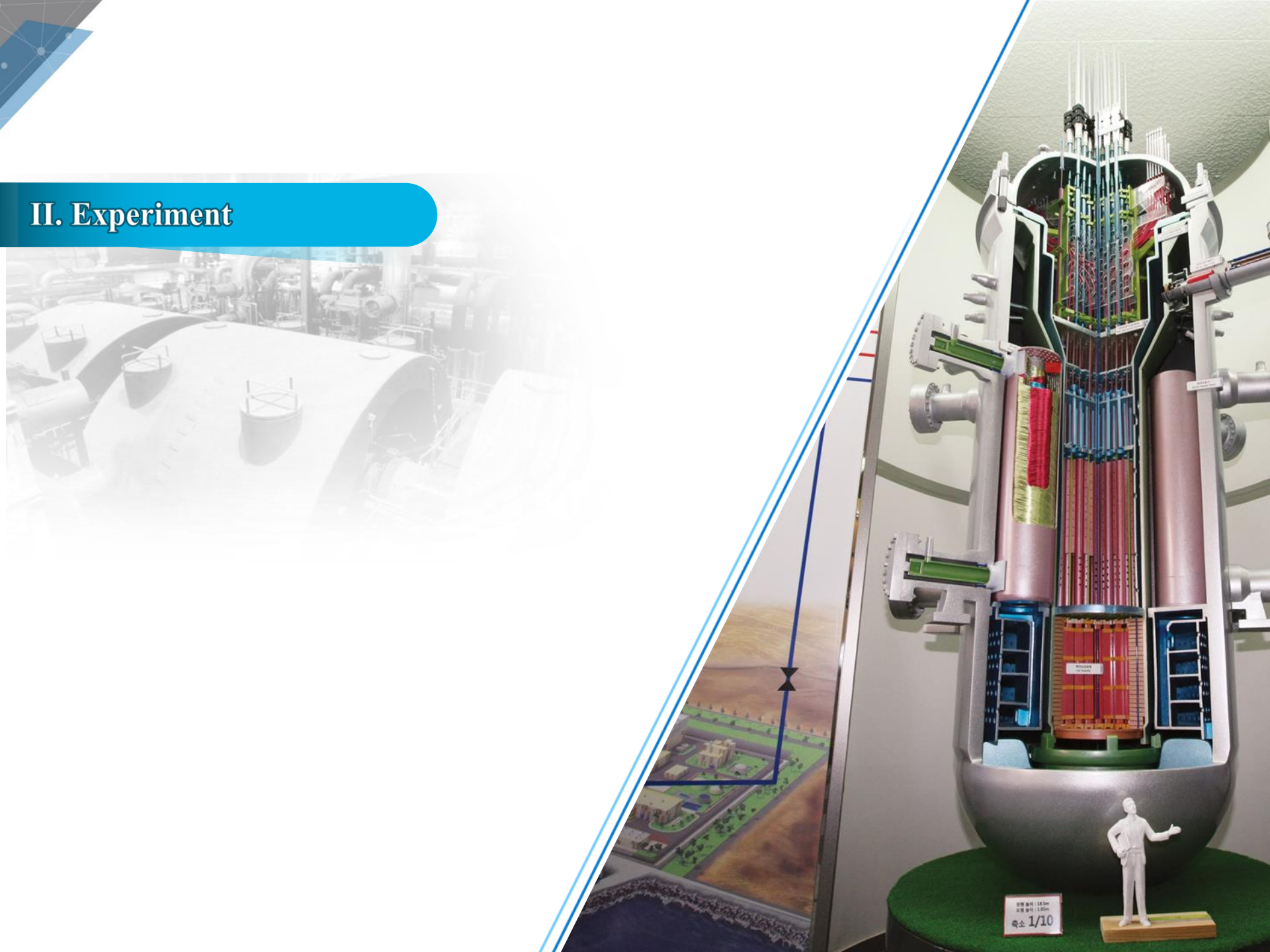
Complex material,
Spent Nuclear Fuel



Simplified
single-element-doped UO_2

Zr^{4+}

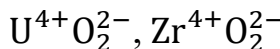
II. Experiment



II. Experiment

Preparation of pellet

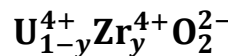
Powder mixing of UO_2 and ThO_2 powder



Pressed into a disk pellet



Sintering at 1700°C for 18 h in a reducing atmosphere with flowing hydrogen

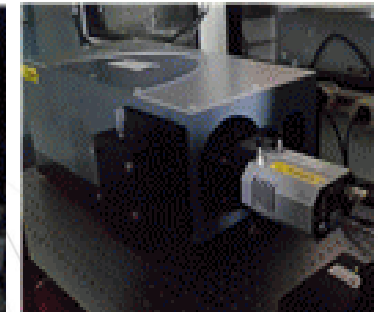
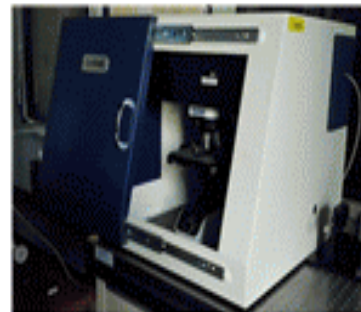


Thickness : < 1 mm
Diameter: ~ 9 mm

XRD (X-Ray Diffraction)

Bruker AXS D8 Advance X-ray Diffractometer using $\text{CuK}\alpha$ radiation at room temperature

Raman spectroscopy



ANDOR Shamrock SR500i spectrometer with a 632.8 nm excitation of He-Ne laser

First-principles DFT calculations

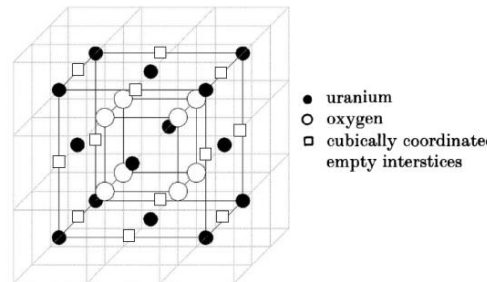
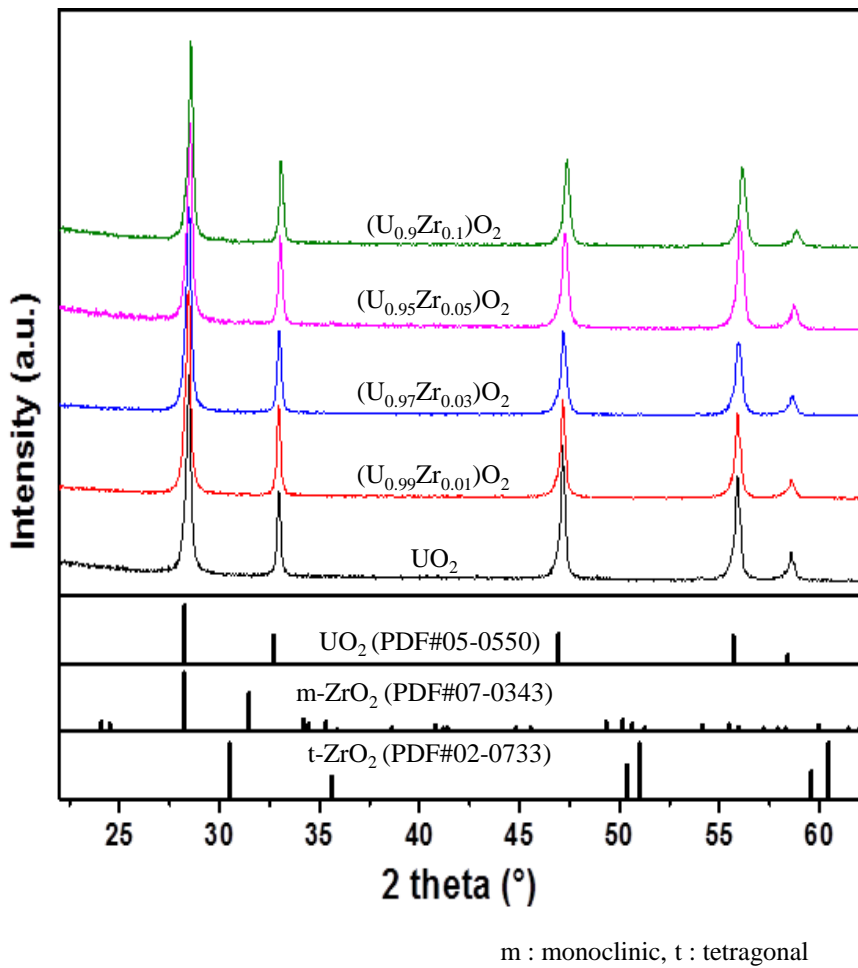
- DFT implemented in VASP
- The projector-augmented wave (PAW) method : represent the core electrons
- The generalized gradient approximation (GGA) with the Perdew-Burke-Ernzerhof (PBE): correct the exchange and correlation potentials
- Energy cut-off of 600 eV were used for all calculations

III. Results & Discussion

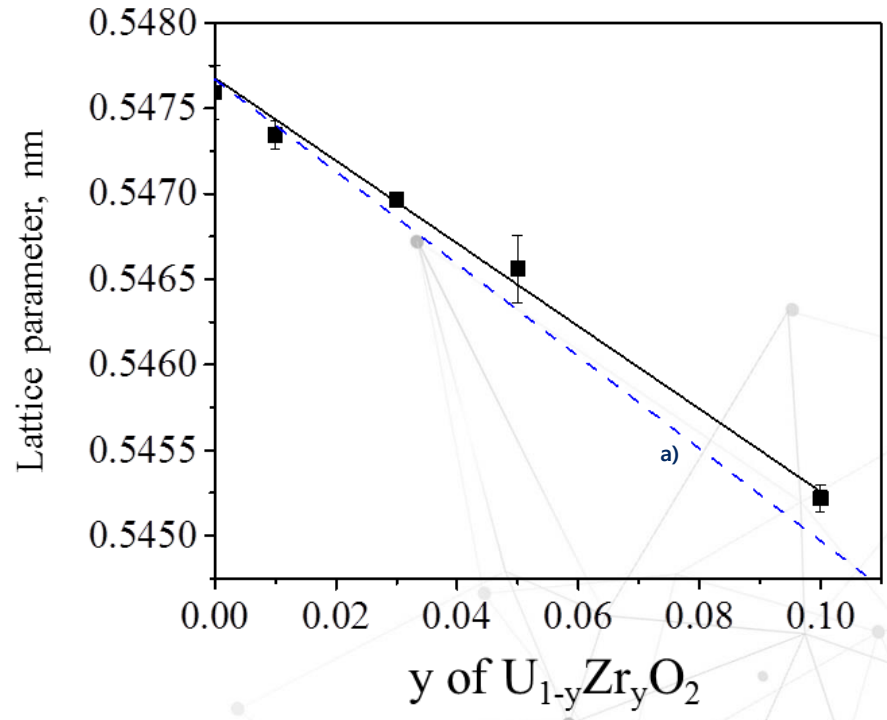


III. Results & Discussion

XRD data of $(U,Zr)O_2$



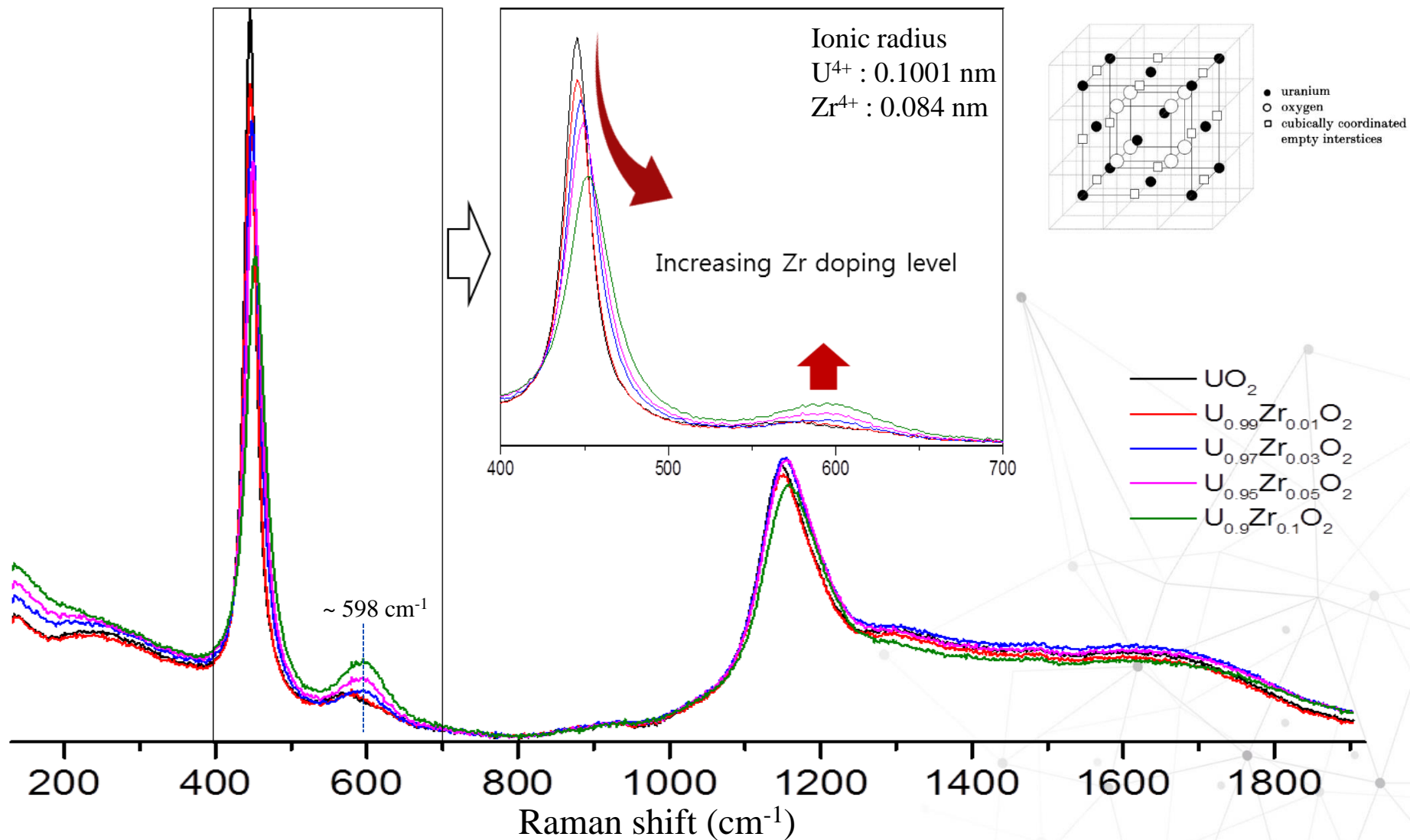
Ionic radius
 $U^{4+} : 0.1001 \text{ nm}$
 $Zr^{4+} : 0.084 \text{ nm}$



a) K. Une *et al.*, J. Am. Ceram. Soc. 66 (1983) C179-C180

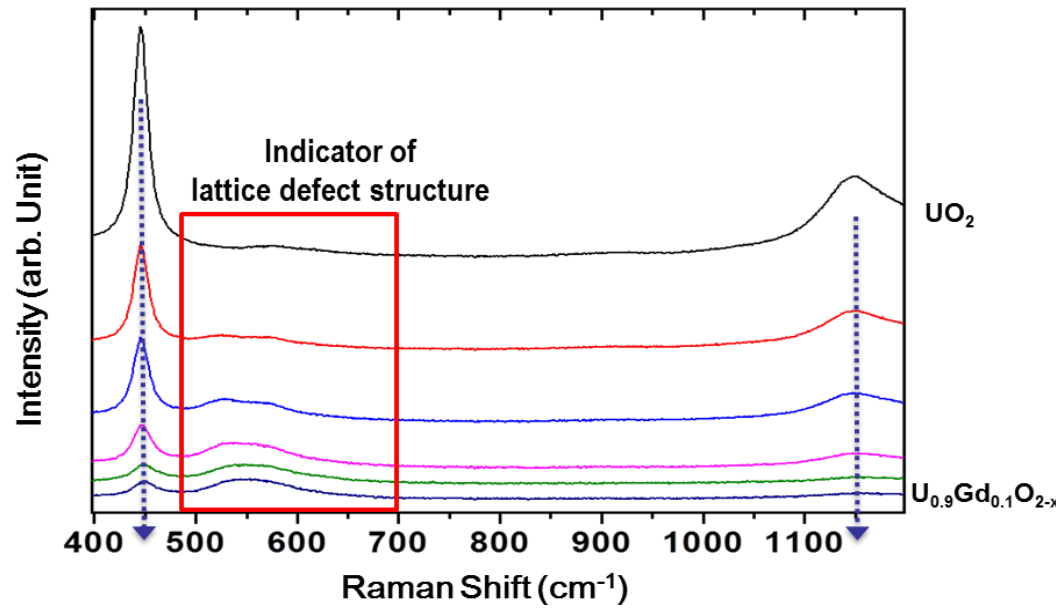
III. Results & Discussion

Raman spectra of $(\text{U}, \text{Zr})\text{O}_2$

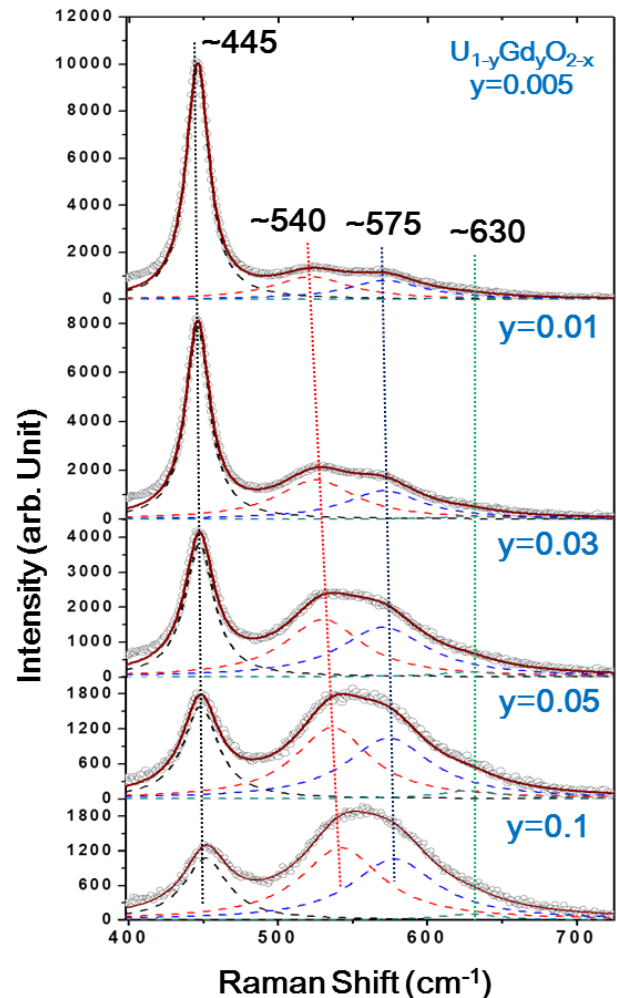


III. Results & Discussion

Raman spectra of $(\text{U}, \text{Gd})\text{O}_2$

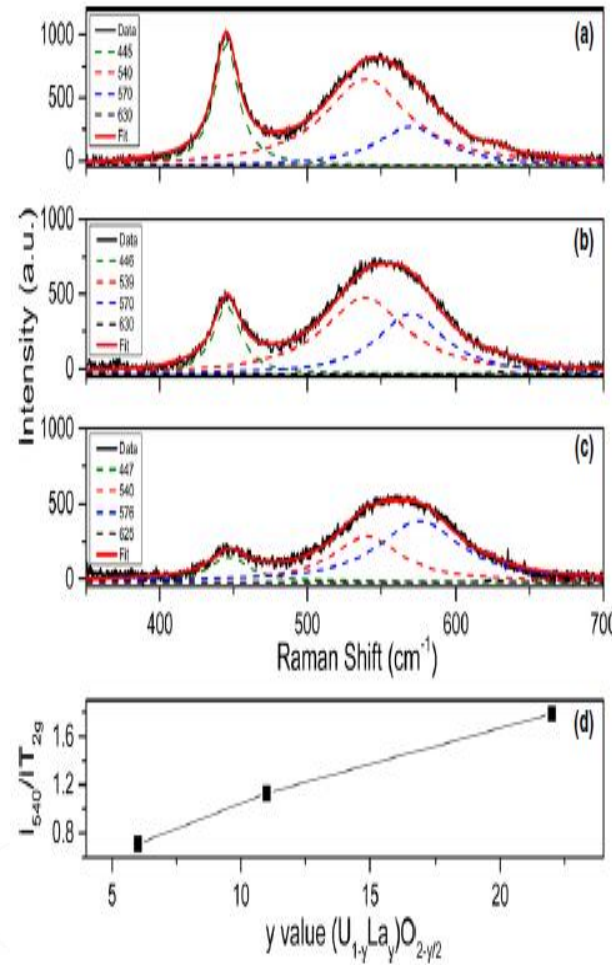
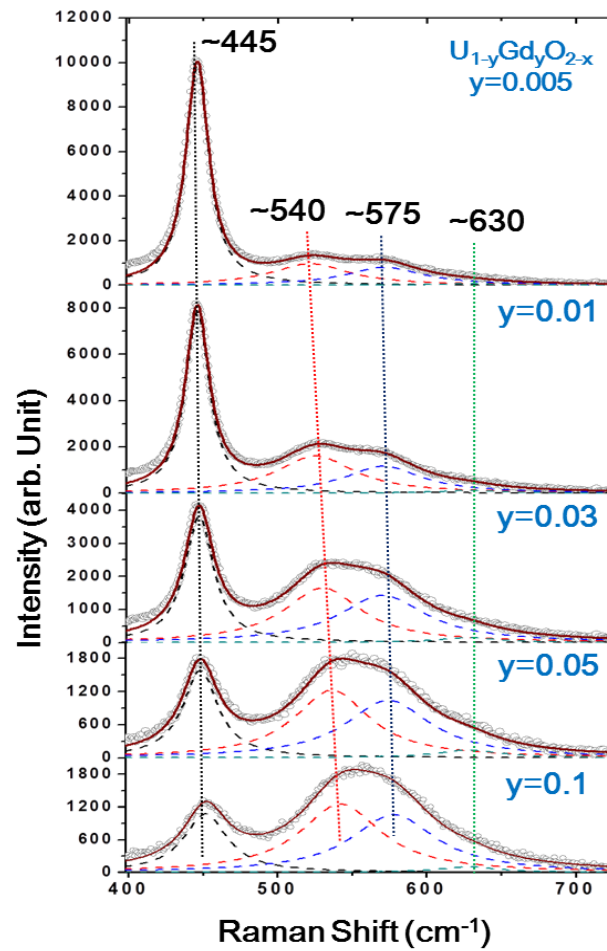
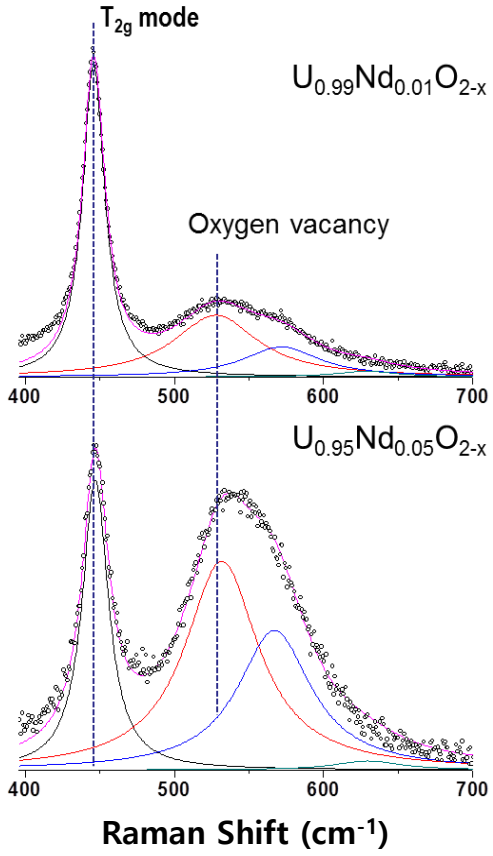


- $\sim 445 \text{ cm}^{-1}$: **T_{2g} fundamental O-U stretch at perfect fluorite structure**
- $\sim 540 \text{ cm}^{-1}$: Lattice distortion from **creation of oxygen vacancies due to Gd³⁺**
- $\sim 575 \text{ cm}^{-1}$: **L-O (Longitudinal-Optical) phonon band**
- $\sim 630 \text{ cm}^{-1}$: Cubooctahedral constituting of the **U_4O_9 phase**
- $\sim 1150 \text{ cm}^{-1}$: **2 L-O phonon**



III. Results & Discussion

Compare with other results

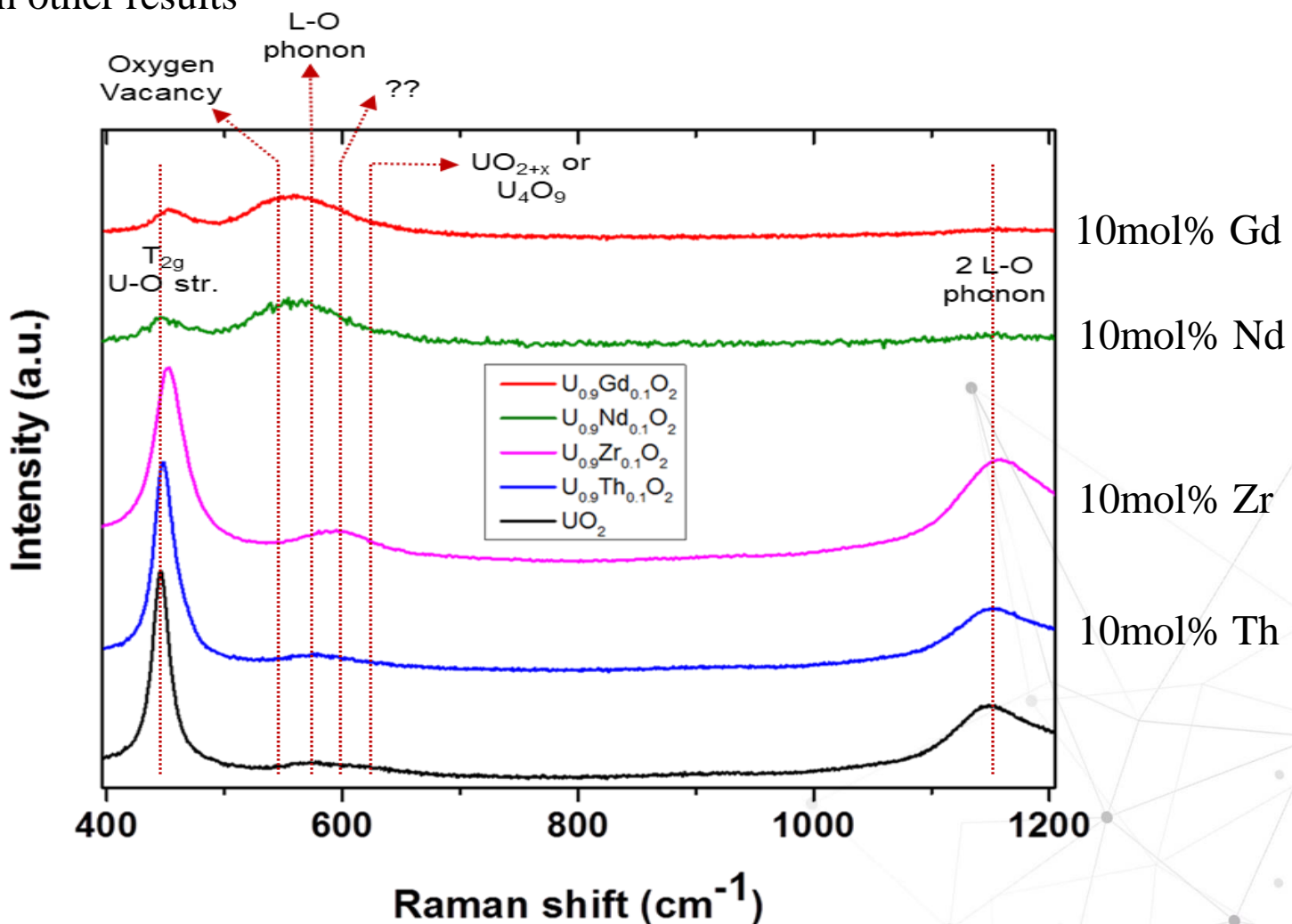


Ln³⁺ doping elements show similar features

$y = 0.06, 0.11, \text{ and } 0.22 \text{ in } \text{U}_{1-y}^{4+}\text{La}_y^{3+}\text{O}_{2-y/2}^{2-}$

III. Results & Discussion

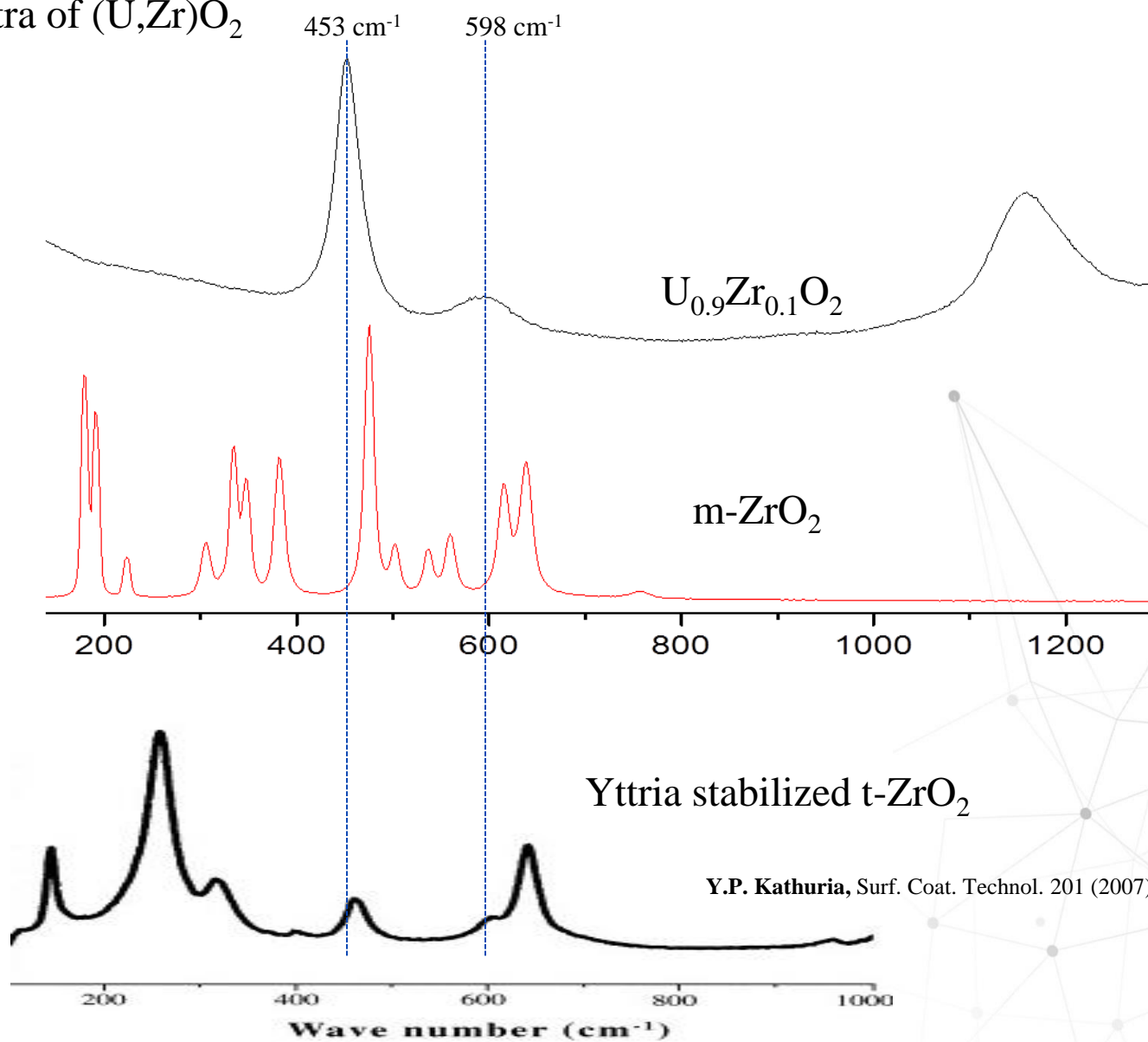
Compare with other results



- J. Lee *et al.*, J. Nucl. Mater. 486 (2017) 216-221
 J. Lee *et al.*, Prog. Nucl. Sci. Technol. 5 (2018) 33-36
 J. Lee *et al.*, Int. J. Energy Res. 43 (2019) 3322-2229
 J. Lee *et al.*, J. Radioanal. Nucl. Chem. 316 (2018) 1295-1300

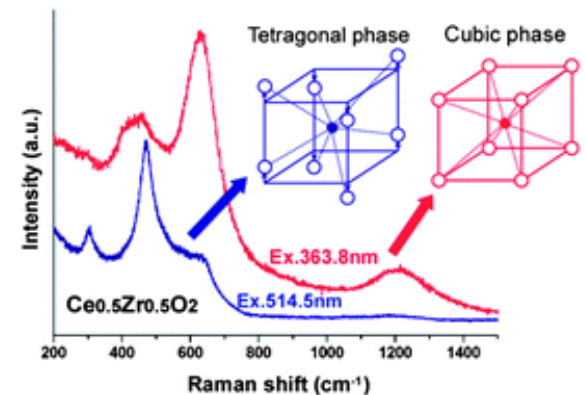
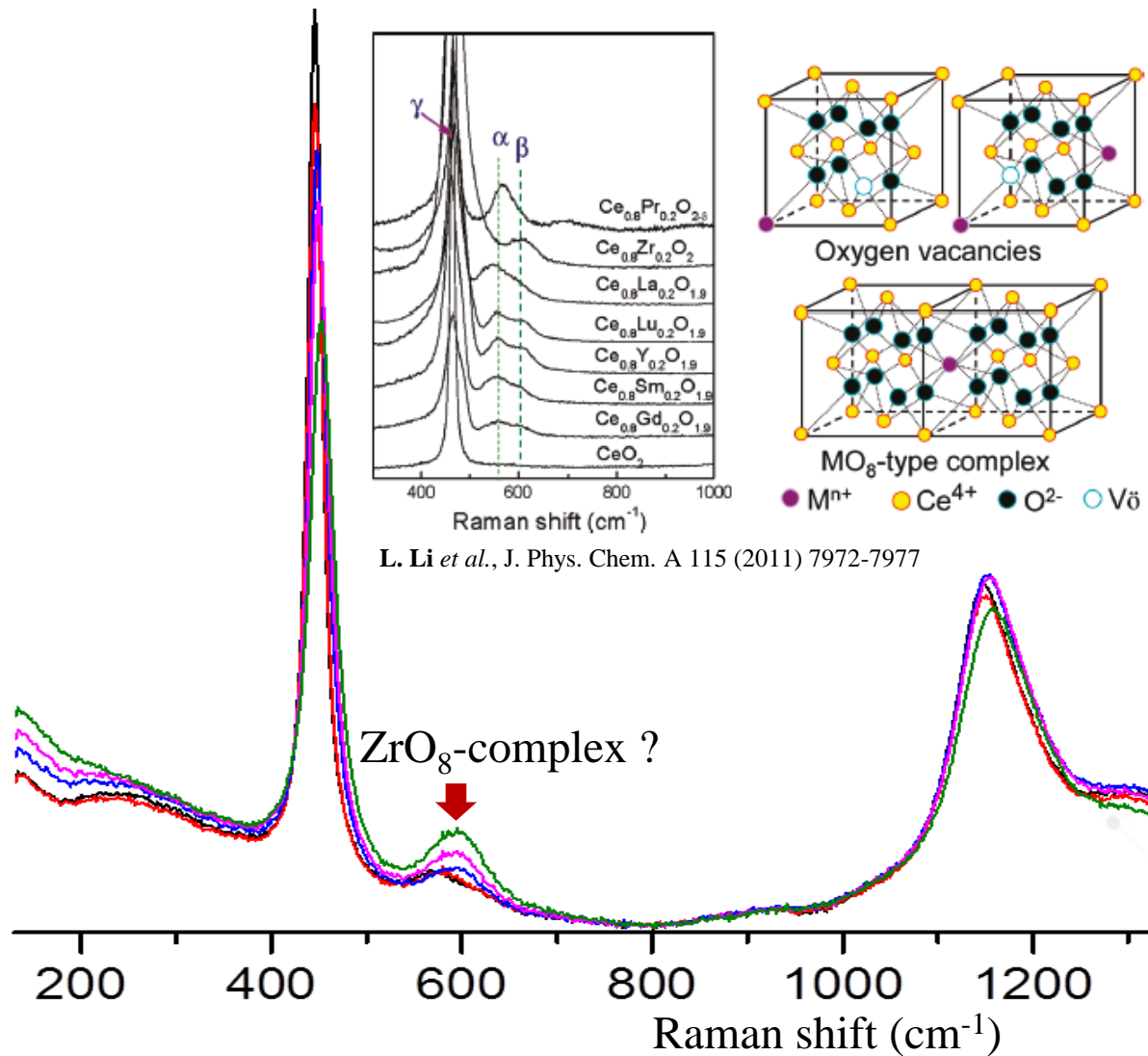
III. Results & Discussion

Raman spectra of $(\text{U}, \text{Zr})\text{O}_2$

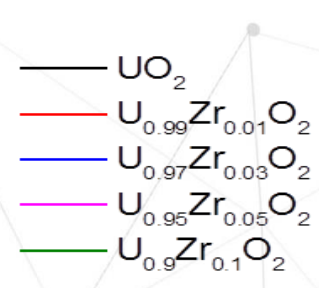


III. Results & Discussion

Raman spectra of $(\text{U}, \text{Zr})\text{O}_2$

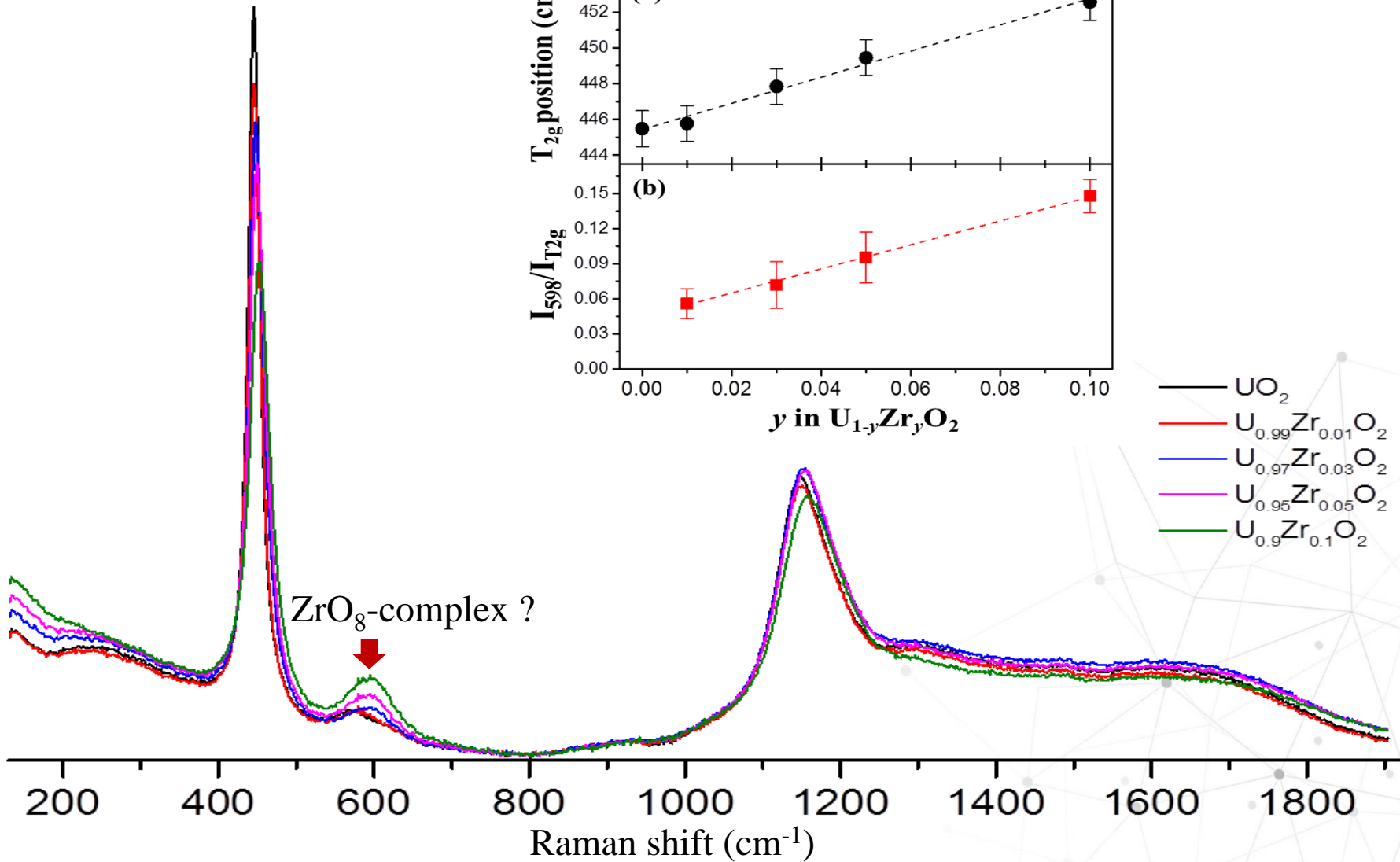


T. Taniguchi et al., Nanoscale 2 (2010) 1426-1428



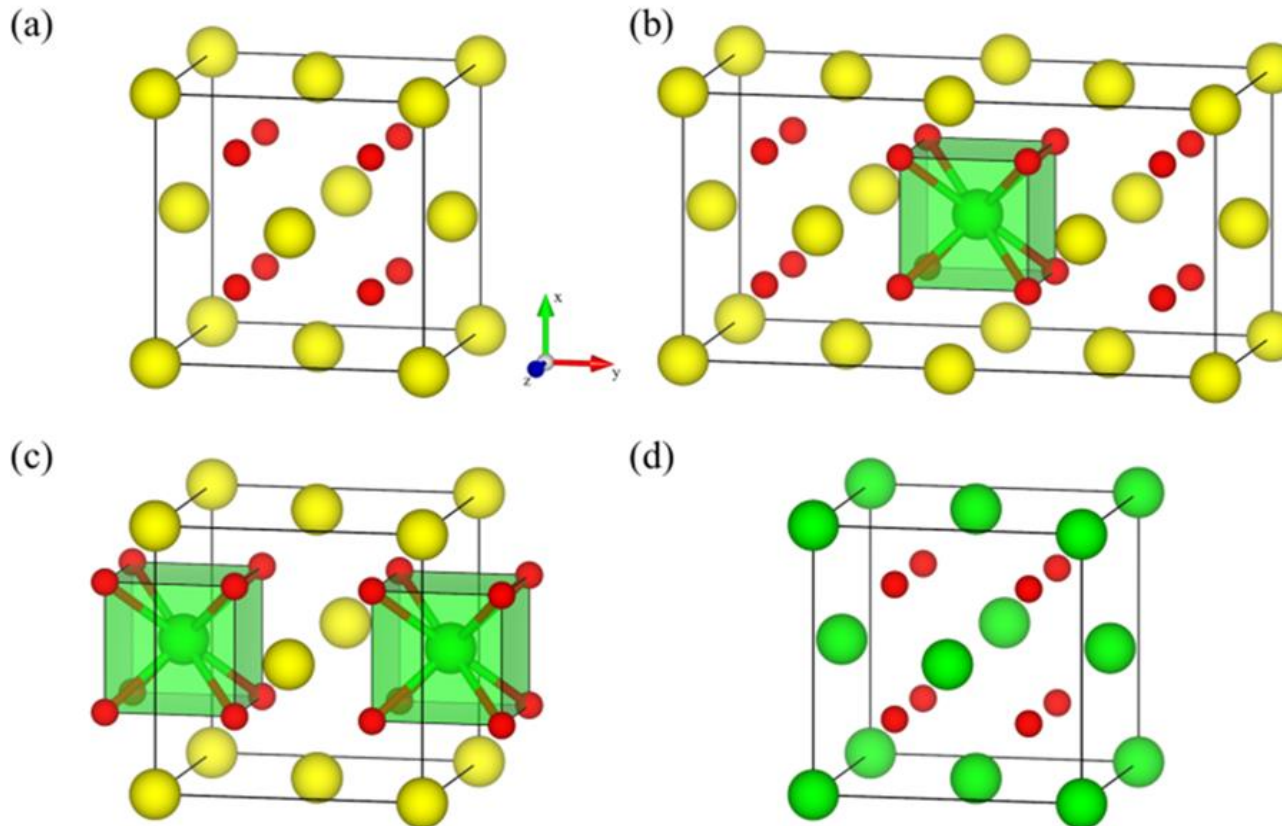
III. Results & Discussion

Raman spectra of $(\text{U}, \text{Zr})\text{O}_2$



III. Results & Discussion

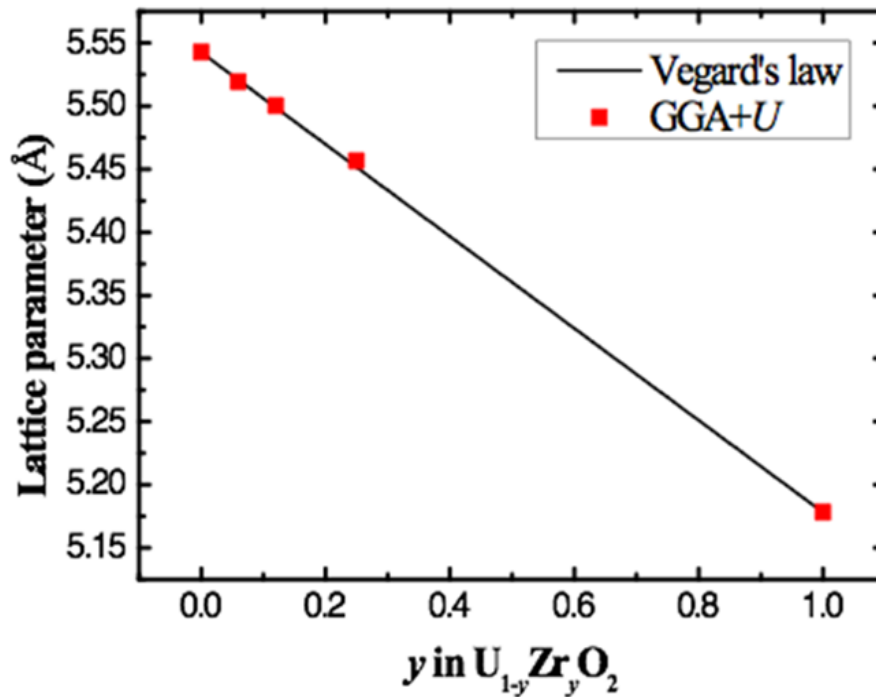
First-principles DFT calculations



Model systems of (a) UO_2 , (b) $\text{U}_{0.87}\text{Zr}_{0.13}\text{O}_2$, (c) $\text{U}_{0.75}\text{Zr}_{0.25}\text{O}_2$, and (d) cubic ZrO_2 .
 The yellow, green, and red spheres represent U, Zr, and O atoms, respectively

III. Results & Discussion

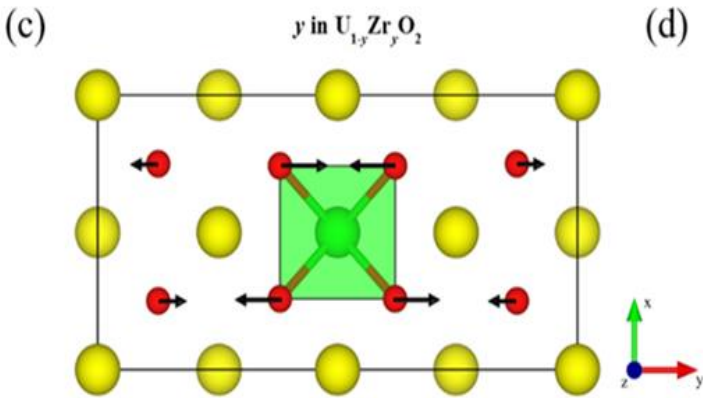
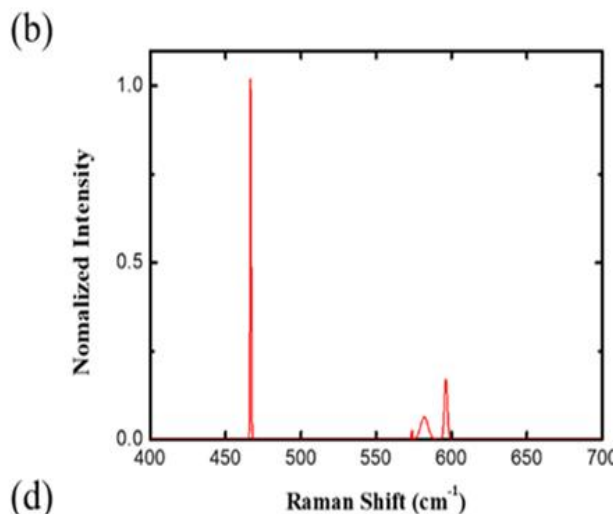
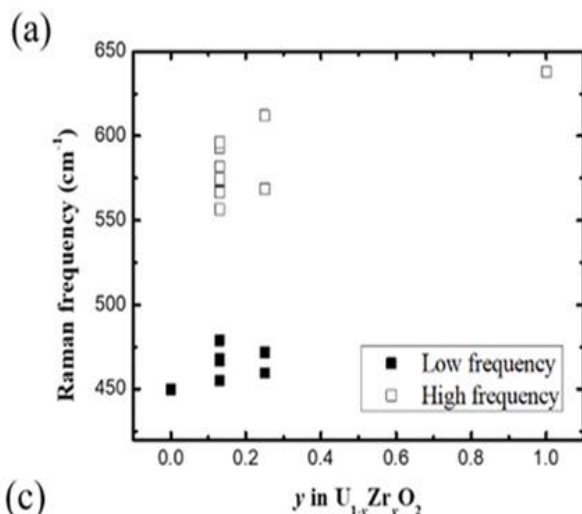
First-principles DFT calculations



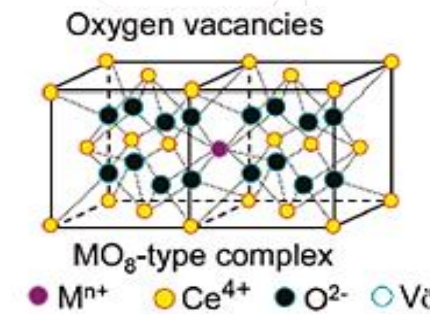
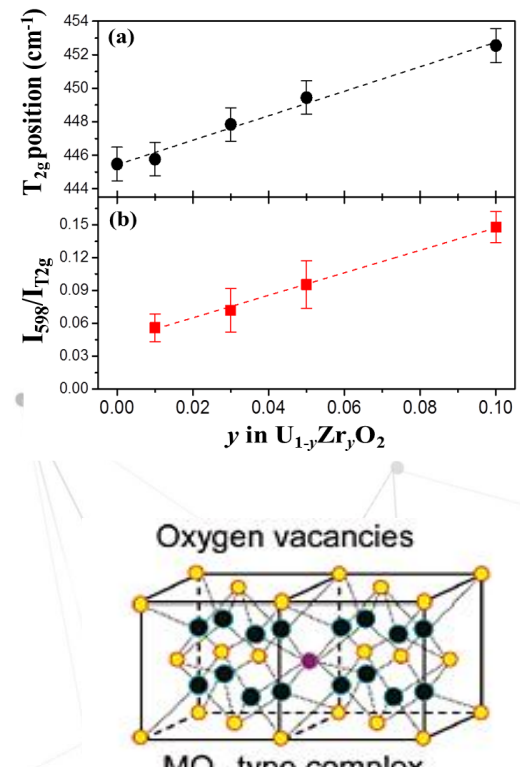
Relationship between the simulated lattice parameter (red squares) calculated using GGA+ U and Zr content (y) in $\text{U}_{1-y}\text{Zr}_y\text{O}_2$ ($y = 0.0, 0.06, 0.13, 0.25$, and 1). This linear relationship obeys Vegard's law (solid black line).

III. Results & Discussion

First-principles DFT calculations



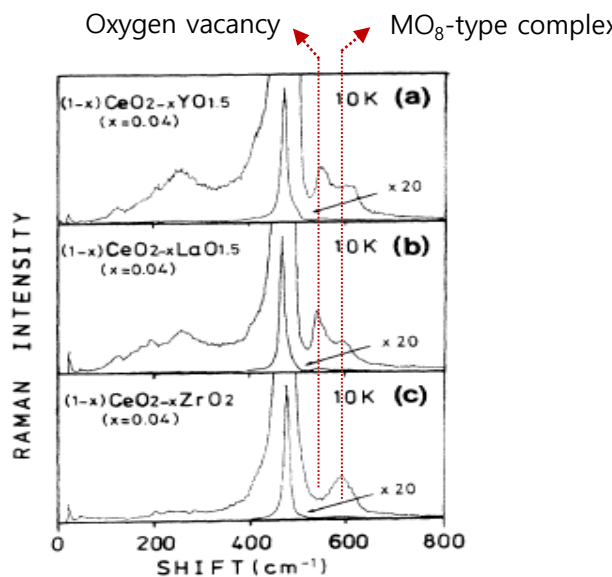
(a) Vibrational frequencies of $\text{U}_{1-y}\text{Zr}_y\text{O}_2$ as a function of Zr composition (y). (b) The simulated intensities and Raman frequencies of $\text{U}_{0.87}\text{Zr}_{0.13}\text{O}_2$. Normal modes of the peaks at (c) 466.82 cm^{-1} and (d) 596.15 cm^{-1} . The yellow, green and red spheres represent U, Zr and O atoms, respectively.



Ionic radius
 $\text{U}^{4+} : 0.1001 \text{ nm}$
 $\text{Zr}^{4+} : 0.084 \text{ nm}$

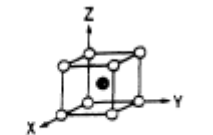
III. Results & Discussion

How about M(III)O₈-type complex?

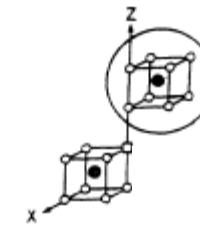


(Ce,Y)O₂

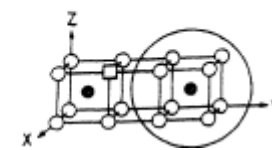
(a)



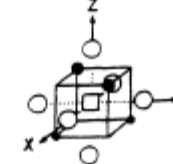
(c)



(b)

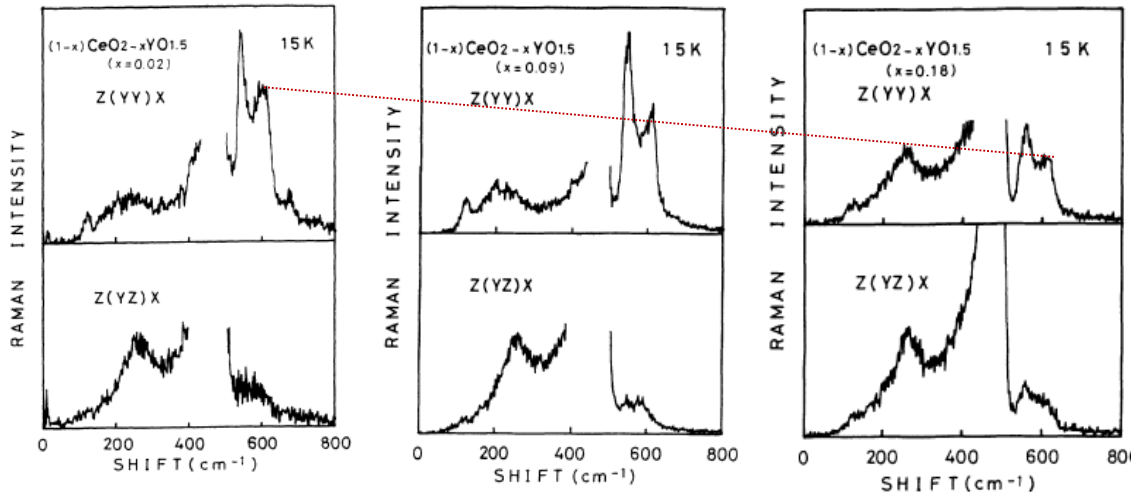


(d)



- O²⁻-vacancy
- O²⁻-ion
- Ce⁴⁺-ion
- Y³⁺-ion

(b), (c), (d) Defect spaces related to oxygen vacancy



The existence of a **MO₈-type complex** :

Dopant M is in 8-fold coordination with O²⁻ (O_h symmetry) excluding oxygen vacancy

Increasing the concentration of Ov :

the space differs from the MO₈-type complex since **the space no longer has O_h symmetry** due to the effect of the neighboring oxygen vacancy.

IV. Summary



IV. Summary

Summary

- The surface structure of $U_{1-y}Zr_yO_2$ pellets have been studied by XRD and Raman spectroscopy
- There is no defect structure related to oxygen vacancy
- The peak at $\sim 598 \text{ cm}^{-1}$ in $U_{1-y}Zr_yO_2$ pellet is supposed to be the existence of ZrO_8 -type complex in UO_2 matrix.
- T_{2g} Raman vibration peak around 445 cm^{-1} shows positive shift and the $I_{598}/I_{T_{2g}}$ linearly increases with increasing Zr doping level
- XRD analysis and Raman spectroscopic observation was consistently supported by first-principles DFT calculation (O in the ZrO_8 -type complex moves longer distance)
- This study could provide important implication for predicting physicochemical properties of a corium (the mixture of core materials, UO_2 and ZrO_2) and reaction product of fuel and cladding

Ongoing and future work

- Electrochemical experiments with $(U,Zr)O_2$
- Experimental characterization integrated with first-principles computational validation on the surface structure of $(U,M^{3+})O_2$



Korea Atomic Energy
Research Institute

Thank you!